Optical imaging of breast cancer oxyhemoglobin flare correlates with neoadjuvant chemotherapy response one day after starting treatment

Darren Roblyer[a,1], Shigeto Ueda[a,1], Albert Cerussi[a], Wendy Tanamai[a], Amanda Durkin[a], Rita Mehta[b], David Hsiang[b], John A. Butler[b], Christine McLaren[b,c], Wen-Pin Chen[b], and Bruce Tromberg[a,2]

[a]Laser Microbeam and Medical Program (LAMMP), Beckman Laser Institute and Medical Clinic, University of California, Irvine, CA 92617; [b]Chao Family Comprehensive Cancer Center, University of California, Irvine Medical Center, Orange, CA 92697; and [c]Department of Epidemiology, University of California, Irvine, CA 92697

Edited* by Rakesh K. Jain, Harvard Medical School and Massachusetts General Hospital, Boston, MA, and approved July 19, 2011 (received for review November 9, 2010)

Approximately 8–20% of breast cancer patients receiving neoadjuvant chemotherapy fail to achieve a measurable response and endure toxic side effects without benefit. Most clinical and imaging measures of response are obtained several weeks after the start of therapy. Here, we report that functional hemodynamic and metabolic information acquired using a noninvasive optical imaging method on the first day after neoadjuvant chemotherapy treatment can discriminate nonresponding from responding patients. Diffuse optical spectroscopic imaging was used to measure absolute concentrations of oxyhemoglobin, deoxyhemoglobin, water, and lipid in tumor and normal breast tissue of 24 tumors in 23 patients with untreated primary breast cancer. Measurements were made before chemotherapy, on day 1 after the first infusion, and frequently during the first week of therapy. Various multidrug, multicycle regimens were used to treat patients. Diffuse optical spectroscopic imaging measurements were compared with final postsurgical pathologic response. A statistically significant increase, or flare, in oxyhemoglobin was observed in partial responding (n = 11) and pathologic complete responding tumors (n = 8) on day 1, whereas nonresponders (n = 5) showed no flare and a subsequent decrease in oxyhemoglobin on day 1. Oxyhemoglobin flare on day 1 was adequate to discriminate nonresponding tumors from responding tumors. Very early measures of chemotherapy response are clinically convenient and offer the potential to alter treatment strategies, resulting in improved patient outcomes.

in vivo imaging | near-infrared | diffuse optics | tissue spectroscopy | therapeutic monitoring

An increasing number of patients diagnosed with locally advanced breast cancer undergo preoperative neoadjuvant chemotherapy (NAC) (1). Although disease-free and overall survival is approximately identical compared with postoperative therapy, primary NAC has been shown to downstage tumor grade and reduce tumor volume, leading to more breast-conserving surgeries (2–4). Patients who experience a pathological complete response (pCR) are associated with longer disease-free and overall survival (2, 5, 6). Unfortunately, between 8% and 20% of patients will have no clinical or pathologic response and will not benefit from months of treatment (2, 7). Noninvasive markers to predict response very early during therapy would help physicians make evidence-based changes to treatment strategies, potentially minimizing side effects and maximizing therapeutic outcome.

Current methods for measuring response, including palpation, mammography, ultrasound, and MRI, have shown limited success (8–11). These methods largely rely on anatomic information, which is generally insensitive to early, functional changes caused by chemotherapy. Alternatively, functional imaging technologies, including contrast-enhanced MRI, magnetic resonance spectroscopy, and 18F-fluorodeoxy-glucose PET (FDG-PET), have shown some predictive capability by monitoring tumor metabolism or perfusion during treatment (12–18). For example, reductions in tumor FDG uptake measured after one cycle of chemotherapy have been shown to be predictive of a favorable outcome (19). Practical limitations, however, may prevent these techniques from being widely applied in clinical practice for this use (20). Current functional imaging modalities require exogenous contrast agents that may be poorly tolerated by some patients and are performed at significant expense (20, 21).

Diffuse optical spectroscopic imaging (DOSI) provides quantitative, functional information from breast tumors in a noninvasive manner using multiwavelength near IR light. Tissue concentrations (ct) of oxygenated hemoglobin (ctO_2Hb), deoxygenated hemoglobin (ctHHb), water (ctH_2O), and lipids as well as tissue oxygen saturation are measured using tomographic imaging instruments (22, 23) and hand-held probes (24–26). Because near IR light is nonionizing, it is possible to use DOSI to monitor physiological changes on a frequent basis without exposing tissue to potentially harmful radiation.

Laboratory and commercial DOSI instruments have been used to characterize both normal and tumor breast tissue (25, 27–29), breast tissue metabolic changes after breast core biopsy (30), and response to neoadjuvant chemotherapy (22, 31–37). Previous neoadjuvant studies have focused on complete pathologic (pCR) response as a primary clinical endpoint and have shown that reductions in ctO_2Hb, ctHHb, and ctH_2O, apparent as early as the first week of primary therapy and continuing until surgery, are predictive of pathologic response (32, 35). These response metrics seem to be consistent between tumors despite chemotherapy regimen and mechanism of action (38).

Author contributions: D.R., S.U., A.C., R.M., D.H., J.A.B., and B.T. designed research; D.R., S.U., A.C., W.T., and A.D. performed research; D.R., S.U., A.C., D.H., C.M., W.-P.C., and B.T. analyzed data; and D.R., S.U., C.M., and B.T. wrote the paper.

Conflict of interest statement: B.T. and A.C. report patents, which are owned by the University of California, that are related to the technology and analysis methods described in this study. The diffuse optical spectroscopic imaging instrumentation used in this study was constructed in a university laboratory using federal grant support (National Institutes of Health). The University of California has licensed diffuse optical spectroscopic imaging technology and analysis methods to two companies, FirstScan, Inc. and Volighten, Inc., for different fields of use, including breast cancer (FirstScan, Inc.). This research was completed without participation, knowledge, or financial support of either company, and data were acquired and processed from patients by coauthors unaffiliated with either entity. The Institutional Review Board and Conflict of Interest Office of the University of California, Irvine, have reviewed both patent and corporate disclosures and did not find any concerns.

*This Direct Submission article had a prearranged editor.

[1]D.R. and S.U. contributed equally to this work.

[2]To whom correspondence should be addressed. E-mail: bjtrombe@uci.edu.

This article contains supporting information online at www.pnas.org/lookup/suppl/doi:10.1073/pnas.1013103108/-/DCSupplemental.

We present here clinical evidence that functional measurements made with DOSI observed the first day after administration of preoperative chemotherapy are predictive of therapy response in patients with primary breast cancer. In contrast to previous NAC studies, we focus here on identifying nonresponding (NR) patients within 1 d of their first infusion. Although the clinical endpoint NR has not been studied as extensively as pCR, the ability to identify these patients very early in treatment has unique implications for rapidly informing treatment strategy alterations.

Results

Table S1 indicates subject and tumor characteristics; 8 of 24 tumors achieved pCR, 11 tumors were classified as partial response (PR), and 5 tumors were classified as NR.

Responding Tumors Show a Flare in ctO_2Hb on Day 1 of Treatment. To determine time points at which diagnostically relevant functional changes occur during the first week of treatment, values of oxyhemoglobin, deoxyhemoglobin, water, and lipids were analyzed in subjects who were measured at least 3 d during the first week of treatment. Table S1 indicates the 17 subjects who met this criterion, and it includes four NR, seven PR, and six pCR tumors. In these subjects, the percent change from baseline of ctO_2Hb was the only optical metric that discriminated responding subjects from nonresponding subjects, and the maximum difference in the mean oxyhemoglobin values between responders and nonresponders occurred on day 1 after the start of therapy. Fig. 1 shows the observed mean percent change from baseline of ctO_2Hb over the first week in responding and nonresponding groups.

Generalized estimating equations (GEE) models that incorporated therapy response, treatment regimen, measurement day, and interaction terms were used to fit the outcomes of oxyhemoglobin, deoxyhemoglobin, water, and lipid changes from baseline. Tumor and normal tissue measurements were modeled separately over the first 7 d of treatment for all 23 subjects. Sensitivity analyses were performed to assess the effect of outlying data points on the model outcomes (*SI Results*). Mean values for percent change from baseline and 95% confidence intervals for the means as predicted by the models for oxyhemoglobin in both tumor and normal tissue are shown in Table 1. All other outcomes are shown in Table S2 and Table S3. At day 1, the differences between the predicted means for NR vs. PR (68.0%) and NR vs. pCR (68.9%) in oxyhemoglobin were larger than corresponding differences at other measurement days, and the 95% confidence intervals for the NR group did not overlap those intervals computed for the PR and pCR groups. The strongest statistical significance for any of the outcomes was found for oxyhemoglobin at day 1 for NR vs. PR (nominal P value = 2.0×10^{-12}, multiple comparisons corrected P value = 2.7×10^{-11}) and NR vs. pCR (nominal P value = 2.5×10^{-6}, corrected P value = 3.6×10^{-5}).

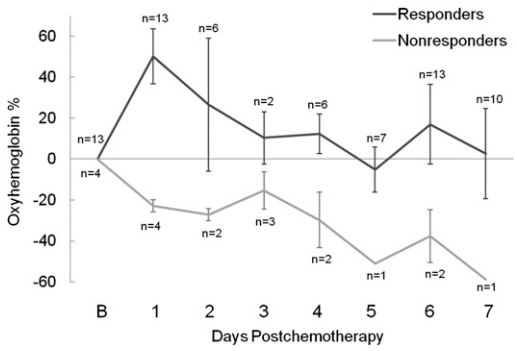

Fig. 1. Percent change in ctO_2Hb during the first 7 d of chemotherapy in responding and nonresponding tumors. The number of tumors measured at each day is indicated. The maximum separation between these groups occurred on day 1. Error bars represent SE.

Treatment type (cytotoxic, cytotoxic and bevacizumab, or cytotoxic and trastuzumab) did not contribute information to the models of percent change from baseline in tumor oxyhemoglobin (score statistic P value = 0.38), deoxyhemoglobin (P = 0.28), lipids (P = 0.069), or water (P = 0.46). Additionally, histology (invasive ductal carcinoma vs. invasive lobular carcinoma), Scarff–Bloom–Richardson grade, c-erbB2 status, estrogen receptor status, progesterone receptor status, age, and body mass index did not show any significant effects on the models (score statistic $0.071 < P < 0.99$ for all) except for age in the outcome of lipids (score statistic P value = 0.039).

In contrast to the tumor tissue, models of normal tissue revealed that the NR group was not simultaneously statistically different from both the PR and pCR groups for any of the measurement days for any outcome. To further explore the paired tumor and normal measurements, the difference between the percent change from baseline for the normal breast and the percent change from baseline for the tumor breast tissue was computed and used as the outcome variable for a GEE model. A near zero estimate for this outcome variable is expected if paired normal and tumor tissue experience the same trends (both in time and magnitude). For oxyhemoglobin, deoxyhemoglobin, water, and lipids, there were multiple measurement days in which the outcome variable was statistically different from zero, which was indicated by the confidence intervals of estimates (Table S4). Despite this result, it is still possible that normal measurements mimicked the temporal behavior of tumor measurements but at a reduced magnitude. For example, for the model outcome of oxyhemoglobin in normal tissue, there was an increase in the PR and pCR groups on day 1 (26.2% and 8.5%, respectively) (Table 1) and a decrease in the NR group (−4.3%), although a pairwise analysis between response groups did not indicate statistically significant differences after correcting for multiple comparisons.

Because the most significant differences between response groups occurred on day 1 after treatment, which was indicated by the GEE analysis, the following results focus on this time point. Fig. 2 shows the observed mean percent change of ctO_2Hb, ctHHb, water, and lipids in all 23 study subjects (24 tumors) on day 1. An increase in ctO_2Hb was observed in both PR (44.5% ± 46.1% SD) and pCR (41.4% ± 39.1% SD) groups, and a decrease was observed in the NR (−22.5% ± 5.10% SD) group. This trend was mirrored in the contralateral normal measurements, with increases in ctO_2Hb in the PR (22.6% ± 43.1% SD) and pCR (12.6% ± 22.0% SD) groups and only small deviations from baseline in the NR (−0.4% ± 9.7% SD) group. Fig. 3 shows absolute molar concentrations of ctO_2Hb in tumors at baseline and day 1 for NR, PR, and pCR groups.

Observed values of tumor ctHHb change were lowest in the NR group (−21.9% ± 17.1% SD) and trended higher in the PR (−5.6% ± 27.5% SD) and pCR groups (9.8% ± 39.3% SD). No trend was observed in ctHHb in contralateral normal tissue, and mean percent change at day 1 was close to zero for all three response groups. Values of water and lipids were not useful to discriminate response groups on day 1 of treatment.

Fig. 4 shows representative ctO_2Hb maps at baseline and day 1 for three different study subjects, one NR, one PR, and one pCR. All of the maps show a 6 × 6-cm measurement area that includes tumor and a surrounding normal margin. The approximate tumor location, determined by ultrasound and palpation, is indicated by a dotted circle. In each example, baseline ctO_2Hb values in the region corresponding to tumor were elevated over

Table 1. Mean values and 95% confidence limits for percent change from baseline for 7 d after the start of chemotherapy in oxyhemoglobin in tumor and normal tissue as predicted by a GEE model

Day	pCR (n = 8)	PR (n = 11)	NR (n = 5)
	Tumor		
1	44.25 (17.89, 70.6)	43.42 (24.12, 62.71)	−24.61 (−34.71, −14.51)
2	−1.4 (−20.46, 17.67)	22.76 (−8.43, 53.96)	−30.22 (−42.86, −17.59)
3	23.01 (6.63, 39.4)	14.81 (−14.59, 44.21)	−20.63 (−41.6, 0.34)
4	−7.52 (−46.74, 31.7)	24.75 (−13.23, 62.72)	−29.22 (−46.29, −12.15)
5	−15.68 (−40.26, 8.9)	16.6 (−17.3, 50.5)	−41.62 (−55.48, −27.77)
6	−4.05 (−21.81, 13.71)	26.2 (−19.9, 72.3)	−37.78 (−55.63, −19.94)
7	−21.55 (−44.96, 1.85)	1.21 (−40.13, 42.54)	−49.38 (−63.24, −35.52)
	Normal		
1	8.5 (−7.85, 24.85)	26.19 (−2.57, 54.96)	−4.33 (−10.5, 1.83)
2	−2.43 (−15.09, 10.23)	3.17 (−11.28, 17.61)	−14.42 (−25.79, −3.05)
3	4.57 (−2.03, 11.17)	−9.74 (−24.19, 4.7)	−13.2 (−22.7, −3.7)
4	−15.05 (−30.15, 0.05)	19.39 (−12.92, 51.7)	−19.78 (−32.3, −7.26)
5	−13.62 (−32.85, 5.6)	7.71 (0.62, 14.8)	−25.33 (−29.2, −21.46)
6	−3.09 (−17.57, 11.39)	6.12 (−8.05, 20.29)	−25.01 (−31.05, −18.97)
7	−16.23 (−36.71, 4.26)	−11.19 (−24.51, 2.14)	−29.78 (−33.65, −25.91)

the surrounding normal tissue, an observation that was previously shown (25).

ctO_2Hb Magnitude and Spatial Extent Discriminate Nonresponders on Day 1 of Therapy. Fig. 5 *Left* shows a scatter plot of tumor ctO_2Hb change from baseline. Perfect separation of NR tumors from both PR and pCR tumors is achieved using the single feature of ctO_2Hb change at day 1.

The spatial extent of elevated oxyhemoglobin was calculated for 16 subjects with sufficiently large measurement areas. The area of elevated ctO_2Hb expanded in PR (57.4% ± 27.7% SD) and pCR (47.7% ± 33.6% SD) subjects and decreased in NR subjects (−33.4% ± 30.3% SD). The change in ctO_2Hb spatial extent is shown in Fig. 5 *Middle*. When magnitude and spatial extent were combined into a single metric, PR subjects experienced a 139.0% ± 114.3% SD increase, pCR subjects experienced an 88.3% ± 62.5% SD increase, and NR subjects experienced a −47.3% ± 23.1% SD decrease in this metric. This combined metric was able to perfectly discriminate NR from PR and pCR, and this finding is shown in Fig. 5 *Right*.

Discussion

We have shown that significant functional changes occur after the first day of preoperative chemotherapy and that these changes are correlated with therapy response. The presence of a flare (increase in magnitude and spatial extent above baseline) in oxyhemoglobin values was indicative of either a partial clinical response or a pathologic complete response. These two patient groups represent individuals who are likely to benefit from improved rates of breast-conserving surgery and/or improved overall and disease-free survival (2–4, 6).

Zhou et al. (33), in collaboration with our group, previously published a case study in which early vascular response was observed in a patient receiving neoadjuvant cytotoxic therapy who had achieved a partial overall response. A transient increase followed by a decrease in blood flow and metabolic rate of oxygen consumption measured using diffuse correlation spectroscopy and DOSI was observed on day 3 of therapy (this subject was not measured on day 1 or 2 of therapy). Others have shown similar findings of early functional changes in animal models using FDG-PET. In three separate studies, an early transient

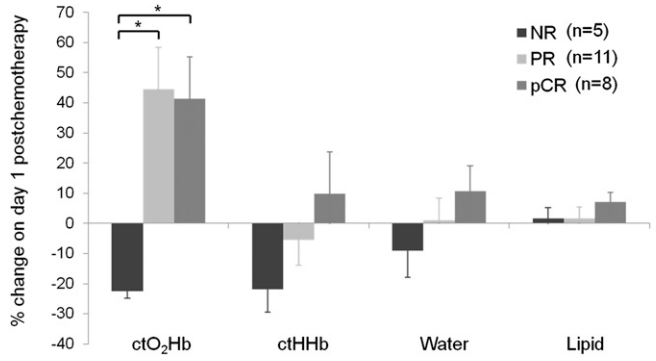

Fig. 2. Percent change in ctO_2Hb, ctHHb, water, and lipids on day 1 compared with baseline. Based on longitudinal GEE models, statistically significant differences, noted with asterisks, were found for NR vs. PR (nominal P value = 3.6×10^{-16}, multiple comparisons corrected P value = 5.0×10^{-15}) and NR vs. pCR (nominal P value = 1.6×10^{-13}, corrected P value = 2.2×10^{-12}), which were adjusted for differences in tissue type and treatment. Error bars represent SE.

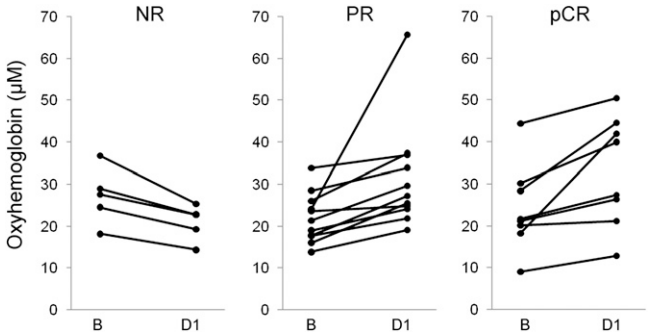

Fig. 3. Absolute values of tumor ctO_2Hb at baseline and day 1 for the different response groups. Baseline and day 1 values in the NR group were 27.2 μM (±6.8 SD) and 20.9 μM (±4.3 SD), respectively, and this represents an average change of −22.5%. Baseline and day 1 values in the PR group were 22.0 μM (±5.9 SD) and 31.5 μM (±12.8 SD), respectively, with an average change of 44.5%. Baseline and day 1 values in the pCR group were 24.1 μM (±10.4 SD) and 33.1 μM (±13.0 SD), respectively, with an average change of 41.4%.

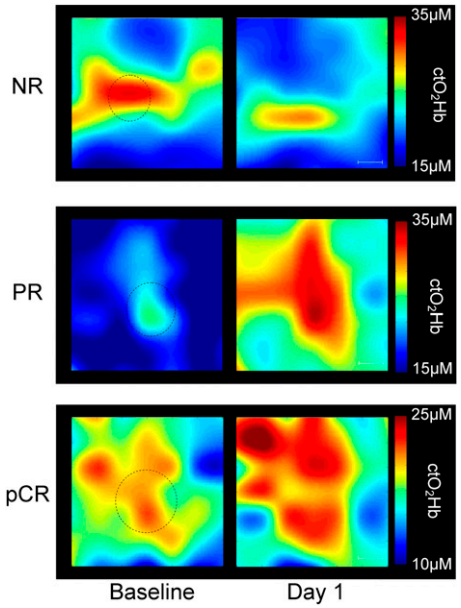

Fig. 4. ctO_2Hb maps from three different subjects at baseline and day 1 after the start of neoadjuvant chemotherapy. Each map shows a 6 × 6-cm measurement area that includes the tumor and a surrounding normal margin. (Scale bar: 1 cm.) The circles represent the location and approximate anatomic size of the tumors determined by ultrasound. (*Top*) An example of a 17-mm tumor that did not respond to chemotherapy. Mean tumor ctO_2Hb dropped 21.6% at day 1, and spatial extent decreased by 54.3%. (*Middle*) An example of a partial response. Tumor was 20 mm before chemotherapy. Mean tumor ctO_2Hb increased 53.1% at day 1, and spatial extent increased by 142.1%. (*Bottom*) An example of a pathologic complete response. Tumor was 30 mm before chemotherapy. Mean tumor ctO_2Hb increased 5.6% at day 1, and spatial extent increased by 4.5%.

increase in tumor FDG uptake was observed during the first week after chemotherapy, independent of tumor growth. This observation was followed by a rapid decrease in FDG uptake and subsequent tumor regression (39–41). The cause of the observed flare was uncertain; it was hypothesized that exposure to chemotherapy transiently induced glucose hypermetabolism in tumors, and cancer cells, inefficiently adapted to the induced metabolic stress, underwent apoptotic cell death through metabolic catastrophe (42, 43).

The biologic origin of the oxyhemoglobin flare in responding subjects observed in this study may stem from one or both of the following factors: (*i*) a rapid decrease in cellular metabolism caused by cytotoxic chemotherapy-induced cell damage and a subsequent decrease in oxyhemoglobin conversion to deoxyhemoglobin, and/or (*ii*) increased perfusion to tissue. Previous investigations have shown significant apoptotic activity and decreased proliferation within 24 h after anthracycline therapy (44–46). A drop in deoxyhemoglobin would also be expected to accompany decreased metabolism; however, only a small drop was observed in the PR group, and an increase was observed in the pCR group.

The response may be better explained by perfusion changes caused by an acute inflammatory response induced by cell damage and death. Previous studies have shown that clinical outcome in breast cancer patients is associated with elevations of proinflammatory serum biomarkers after taxane treatment (47–50). Tumor cell exposure to anthracyclines and some platin drugs has been shown to induce immunostimulatory apoptosis and presentation of damage-associated molecular patterns, including calreticulin, heat-shock proteins, and high-mobility group box 1 proteins, before, during, or after apoptosis (51–54). These damage-associated molecular patterns signal the release of proinflammatory cytokines and inflammatory molecules, including IL-1, IL-6, TNFα, nitric oxide, and histamine, which stimulate innate and adaptive immunity and induce vascular changes. The vascular hallmarks of acute inflammation include increased vascular permeability and vessel dilation, which transiently increases perfusion to the injured area over the course of hours to days (55–57). Although DOSI does not directly measure blood flow, the concomitant increase in total hemoglobin observed during oxyhemoglobin flare does suggest an increase in perfusion.

NR patients may not elicit the same immune response because of a higher proportion of chemoresistant or nonimmunostimulatory tumor cells. Additionally, NR patients may have severely limited perfusion and be especially devoid of vascular reactivity because of loss of smooth muscle cell coverage and innervations (58). This loss could also inhibit drug-induced cell/vascular damage and subsequent inflammatory flare.

Measurements from the contralateral normal breasts support the idea of a systemic or tissue-specific vascular/inflammatory response. Although not statistically significant, responding subjects seemed to exhibit an oxyhemoglobin flare in the contralateral normal breast, whereas nonresponding subjects showed almost no change at day 1. The magnitude of the flare in the normal breast was reduced compared with tumor measurements. The magnitude of oxyhemoglobin flare in both tumor and contralateral normal tissue may reflect individual subject vascular and immune responsiveness to cellular stress, which might be closely related to chemosensitivity. It is also of note that, because DOSI measurements represent the average optical properties of the measurement volume, it is possible that surrounding normal tissue may contribute to the observed flare in tumor locations.

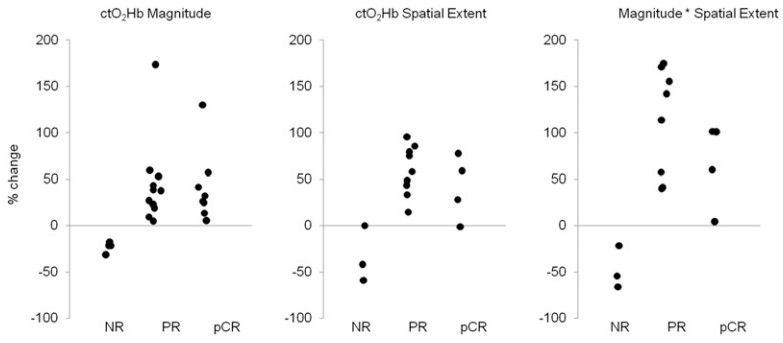

Fig. 5. Percent change in ctO_2Hb magnitude (concentration), spatial extent, and magnitude × spatial extent for NR, PR, and pCR tumors. In all three cases, perfect separation was achieved between nonresponding and responding tumors.

This study is limited because of the small number of subjects and lack of additional confirmatory methods. The additional measurements of glucose metabolism, blood flow, and inflammatory markers would help to elucidate the underlying biological basis of flare response. Another limitation of this study is that several different therapy regimens were explored. It is of note, however, that the flare reaction seemed to be indicative of response regardless of age, body mass index, and tumor subtypes, and no differences were seen between treatment regimens. It should be emphasized that this study was retrospective and correlative in nature, and future prospective validations are necessary to confirm the predictive nature of oxyhemoglobin flare.

In conclusion, we observed a significant tumor ctO_2Hb flare reaction on the first day after neoadjuvant chemotherapy in responding subjects. This flare was adequate to perfectly discriminate nonresponding subjects from both partial and pathologic complete responders. Furthermore, the majority of responding subjects showed ctO_2Hb flare in the contralateral normal breast, whereas nonresponding subjects did not. The implementation of these measurements in the clinic may be used to monitor and strategically alter treatment strategies for breast cancer patients by rapidly identifying likely nonresponders. This implementation could lead to the development of new approaches for managing patients and expediently assessing chemosensitivity for individual subjects.

Materials and Methods

A detailed description of materials and methods is available in *SI Materials and Methods*.

Briefly, DOSI, which is a near IR optical imaging technique, was used to measure tissue concentrations of oxyhemoglobin, deoxyhemoglobin, water, and lipids in breast cancer patients undergoing neoadjuvant chemotherapy (Fig. S1). Changes in the magnitude and spatial dynamics of these quantities in tumor and normal breast tissue were statistically compared with overall response to chemotherapy in 23 subjects with 24 tumors. The GEE method was used to analyze the correlation between values for oxyhemoglobin, deoxyhemoglobin, water, and lipids measured on different days for individual subjects. Treatment response was stratified into a tertiary classification scheme of pCR, PR, and NR. Subjects with no residual carcinoma after therapy were considered pCR. Subjects with a 50% or greater reduction in tumor size determined from the maximum tumor dimensions were considered PR, and subjects with a less than 50% reduction were considered NR. All subjects provided informed consent and participated in this study under a clinical protocol approved by the Institutional Review Board at the University of California, Irvine (02-2306).

ACKNOWLEDGMENTS. The authors wish to thank Montana Compton for her assistance, as well as the subjects who generously volunteered their time for this study. This work was supported by National Institutes of Health Grants P41-RR01192 (Laser Microbeam and Medical Program), U54-CA105480 (Network for Translational Research in Optical Imaging), U54-CA136400, R01-CA142989, NCI-2P30CA62203 (University of California, Irvine Cancer Center Support Grant), and NCI-T32CA009054 (University of California, Irvine Institutional Training Grant). Beckman Laser Institute programmatic support from Beckman Foundation and Air Force Research Laboratory Agreement Number FA9550-04-1-0101 is acknowledged.

1. Kaufmann M, et al. (2007) Recommendations from an international expert panel on the use of neoadjuvant (primary) systemic treatment of operable breast cancer: New perspectives 2006. *Ann Oncol* 18:1927–1934.
2. Rastogi P, et al. (2008) Preoperative chemotherapy: Updates of National Surgical Adjuvant Breast and Bowel Project Protocols B-18 and B-27. *J Clin Oncol* 26:778–785.
3. Wolff AC, et al. (2008) Research issues affecting preoperative systemic therapy for operable breast cancer. *J Clin Oncol* 26:806–813.
4. Gralow JR, et al. (2008) Preoperative therapy in invasive breast cancer: Pathologic assessment and systemic therapy issues in operable disease. *J Clin Oncol* 26:814–819.
5. Fisher ER, et al. (2002) Pathobiology of preoperative chemotherapy: Findings from the National Surgical Adjuvant Breast and Bowel (NSABP) protocol B-18. *Cancer* 95: 681–695.
6. Symmans WF, et al. (2007) Measurement of residual breast cancer burden to predict survival after neoadjuvant chemotherapy. *J Clin Oncol* 25:4414–4422.
7. Caudle AS, et al. (2010) Predictors of tumor progression during neoadjuvant chemotherapy in breast cancer. *J Clin Oncol* 28:1821–1828.
8. Yeh E, et al. (2005) Prospective comparison of mammography, sonography, and MRI in patients undergoing neoadjuvant chemotherapy for palpable breast cancer. *AJR Am J Roentgenol* 184:868–877.
9. Mankoff DA, et al. (1999) Monitoring the response of patients with locally advanced breast carcinoma to neoadjuvant chemotherapy using [technetium 99m]-sestamibi scintimammography. *Cancer* 85:2410–2423.
10. Tardivon AA, Ollivier L, El Khoury C, Thibault F (2006) Monitoring therapeutic efficacy in breast carcinomas. *Eur Radiol* 16:2549–2558.
11. Chen JH, et al. (2009) Impact of MRI-evaluated neoadjuvant chemotherapy response on change of surgical recommendation in breast cancer. *Ann Surg* 249:448–454.
12. Smith IC, et al. (2000) Positron emission tomography using [(18)F]-fluorodeoxy-D-glucose to predict the pathologic response of breast cancer to primary chemotherapy. *J Clin Oncol* 18:1676–1688.
13. Emmering J, et al. (2008) Preoperative [18F] FDG-PET after chemotherapy in locally advanced breast cancer: Prognostic value as compared with histopathology. *Ann Oncol* 19:1573–1577.
14. Rousseau C, et al. (2006) Monitoring of early response to neoadjuvant chemotherapy in stage II and III breast cancer by [18F]fluorodeoxyglucose positron emission tomography. *J Clin Oncol* 24:5366–5372.
15. Martoni AA, et al. (2010) Early (18)F-2-fluoro-2-deoxy-d-glucose positron emission tomography may identify a subset of patients with estrogen receptor-positive breast cancer who will not respond optimally to preoperative chemotherapy. *Cancer* 116: 805–813.
16. Schwarz-Dose J, et al. (2009) Monitoring primary systemic therapy of large and locally advanced breast cancer by using sequential positron emission tomography imaging with [18F]fluorodeoxyglucose. *J Clin Oncol* 27:535–541.
17. Schelling M, et al. (2000) Positron emission tomography using [(18)F]Fluorodeoxyglucose for monitoring primary chemotherapy in breast cancer. *J Clin Oncol* 18: 1689–1695.
18. Baek HM, et al. (2009) Predicting pathologic response to neoadjuvant chemotherapy in breast cancer by using MR imaging and quantitative 1H MR spectroscopy. *Radiology* 251:653–662.
19. Berriolo-Riedinger A, et al. (2007) [18F]FDG-PET predicts complete pathological response of breast cancer to neoadjuvant chemotherapy. *Eur J Nucl Med Mol Imaging* 34:1915–1924.
20. Facey K, Bradbury I, Laking G, Payne E (2007) Overview of the clinical effectiveness of positron emission tomography imaging in selected cancers. *Health Technol Assess* 11: iii–267.
21. Gilbert FJ (2008) Breast cancer screening in high risk women. *Cancer Imaging* 8:S6–S9.
22. Choe R, et al. (2005) Diffuse optical tomography of breast cancer during neoadjuvant chemotherapy: A case study with comparison to MRI. *Med Phys* 32:1128–1139.
23. Pogue BW, et al. (2001) Quantitative hemoglobin tomography with diffuse near-infrared spectroscopy: Pilot results in the breast. *Radiology* 218:261–266.
24. Bevilacqua F, Berger AJ, Cerussi AE, Jakubowski D, Tromberg BJ (2000) Broadband absorption spectroscopy in turbid media by combined frequency-domain and steady-state methods. *Appl Opt* 39:6498–6507.
25. Cerussi A, et al. (2006) In vivo absorption, scattering, and physiologic properties of 58 malignant breast tumors determined by broadband diffuse optical spectroscopy. *J Biomed Opt* 11:044005.
26. Tromberg BJ, et al. (2005) Imaging in breast cancer: Diffuse optics in breast cancer: Detecting tumors in pre-menopausal women and monitoring neoadjuvant chemotherapy. *Breast Cancer Res* 7:279–285.
27. Shah N, et al. (2004) Spatial variations in optical and physiological properties of healthy breast tissue. *J Biomed Opt* 9:534–540.
28. Durduran T, et al. (2002) Bulk optical properties of healthy female breast tissue. *Phys Med Biol* 47:2847–2861.
29. Zhu Q, et al. (2010) Early-stage invasive breast cancers: Potential role of optical tomography with US localization methods. *Radiology* 256:367–378.
30. Tanamai W, et al. (2009) Diffuse optical spectroscopy measurements of healing in breast tissue after core biopsy: Case study. *J Biomed Opt* 14:014024.
31. Jakubowski DB, et al. (2004) Monitoring neoadjuvant chemotherapy in breast cancer using quantitative diffuse optical spectroscopy: A case study. *J Biomed Opt* 9:230–238.
32. Cerussi A, et al. (2007) Predicting response to breast cancer neoadjuvant chemotherapy using diffuse optical spectroscopy. *Proc Natl Acad Sci USA* 104:4014–4019.
33. Zhou C, et al. (2007) Diffuse optical monitoring of blood flow and oxygenation in human breast cancer during early stages of neoadjuvant chemotherapy. *J Biomed Opt* 12:051903.
34. Cerussi AE, et al. (2010) Frequent optical imaging during breast cancer neoadjuvant chemotherapy reveals dynamic tumor physiology in an individual patient. *Acad Radiol* 17:1031–1039.
35. Soliman H, et al. (2010) Functional imaging using diffuse optical spectroscopy of neoadjuvant chemotherapy response in women with locally advanced breast cancer. *Clin Cancer Res* 16:2605–2614.
36. Jiang S, et al. (2009) Evaluation of breast tumor response to neoadjuvant chemotherapy with tomographic diffuse optical spectroscopy: Case studies of tumor region-of-interest changes. *Radiology* 252:551–560.
37. Zhu Q, et al. (2008) Noninvasive monitoring of breast cancer during neoadjuvant chemotherapy using optical tomography with ultrasound localization. *Neoplasia* 10: 1028–1040.
38. Tromberg BJ, Cerussi AE (2010) Imaging breast cancer chemotherapy response with light. Commentary on Soliman et al., p. 2605. *Clin Cancer Res* 16:2486–2488.

39. Aliaga A, et al. (2007) A small animal positron emission tomography study of the effect of chemotherapy and hormonal therapy on the uptake of 2-deoxy-2-[F-18] fluoro-D-glucose in murine models of breast cancer. *Mol Imaging Biol* 9:144–150.
40. Aide N, et al. (2009) Early evaluation of the effects of chemotherapy with longitudinal FDG small-animal PET in human testicular cancer xenografts: Early flare response does not reflect refractory disease. *Eur J Nucl Med Mol Imaging* 36:396–405.
41. Bjurberg M, et al. (2009) Early changes in 2-deoxy-2-[18F]fluoro-D-glucose metabolism in squamous-cell carcinoma during chemotherapy in vivo and in vitro. *Cancer Biother Radiopharm* 24:327–332.
42. Jones RG, Thompson CB (2009) Tumor suppressors and cell metabolism: A recipe for cancer growth. *Genes Dev* 23:537–548.
43. Jin S, DiPaola RS, Mathew R, White E (2007) Metabolic catastrophe as a means to cancer cell death. *J Cell Sci* 120:379–383.
44. Archer CD, et al. (2003) Early changes in apoptosis and proliferation following primary chemotherapy for breast cancer. *British Journal of Cancer* 89:1035–1041.
45. Buchholz TA, et al. (2003) Chemotherapy-induced apoptosis and Bcl-2 levels correlate with breast cancer response to chemotherapy. *Cancer J* 9:33–41.
46. Buchholz TA, et al. (2005) The nuclear transcription factor kappaB/bcl-2 pathway correlates with pathologic complete response to doxorubicin-based neoadjuvant chemotherapy in human breast cancer. *Clin Cancer Res* 11:8398–8402.
47. Mills PJ, et al. (2008) Predictors of inflammation in response to anthracycline-based chemotherapy for breast cancer. *Brain Behav Immun* 22:98–104.
48. Nolen BM, et al. (2008) Serum biomarker profiles and response to neoadjuvant chemotherapy for locally advanced breast cancer. *Breast Cancer Res* 10:R45.
49. Pusztai L, et al. (2004) Changes in plasma levels of inflammatory cytokines in response to paclitaxel chemotherapy. *Cytokine* 25:94–102.
50. Tsavaris N, Kosmas C, Vadiaka M, Kanelopoulos P, Boulamatsis D (2002) Immune changes in patients with advanced breast cancer undergoing chemotherapy with taxanes. *Br J Cancer* 87:21–27.
51. Green DR, Ferguson T, Zitvogel L, Kroemer G (2009) Immunogenic and tolerogenic cell death. *Nat Rev Immunol* 9:353–363.
52. Obeid M, et al. (2007) Calreticulin exposure dictates the immunogenicity of cancer cell death. *Nat Med* 13:54–61.
53. Zitvogel L, Apetoh L, Ghiringhelli F, Kroemer G (2008) Immunological aspects of cancer chemotherapy. *Nat Rev Immunol* 8:59–73.
54. Apetoh L, Mignot G, Panaretakis T, Kroemer G, Zitvogel L (2008) Immunogenicity of anthracyclines: Moving towards more personalized medicine. *Trends Mol Med* 14: 141–151.
55. Ryan GB, Majno G (1977) Acute inflammation. A review. *Am J Pathol* 86:183–276.
56. Gabay C, Kushner I (1999) Acute-phase proteins and other systemic responses to inflammation. *N Engl J Med* 340:448–454.
57. Wilhelm DL (1973) Mechanisms responsible for increased vascular permeability in acute inflammation. *Agents Actions* 3:297–306.
58. Teicher BA, Ellis LM, eds (2008) *Antiangiogenic Agents in Cancer Therapy Series: Cancer Drug Discovery and Development* (Humana Press, Totowa, NJ), 2nd Ed.

Supporting Information

Roblyer et al. 10.1073/pnas.1013103108

SI Materials and Methods

Diffuse Optical Spectroscopic Imaging Instrumentation. Design details and concepts of the diffuse optical spectroscopic imaging (DOSI) system are described elsewhere (1–3). Briefly, the instrument uses both frequency domain and continuous wave (CW) spectroscopy measurements in the near IR spectrum (650–1,000 nm) to determine the tissue optical scattering and absorption properties. Six diode laser sources (660, 680, 780, 810, 830, and 850 nm) are used for frequency domain illumination and are intensity-modulated between 50 and 500 MHz. Amplitude and phase of the detected signals are input into an analytical model of diffuse light transport to determine tissue scattering and absorption coefficients at these wavelengths. White light illumination is used for continuous wave spectroscopy; detected reflectance spectra are fit and scaled to frequency domain measurements so that absorption is determined continuously over the entire spectral range. Absolute tissue concentrations are calculated by using the Beer–Lambert law and known extinction coefficient spectra of deoxyhemoglobin (HHb), oxyhemoglobin (HbO_2), water, and lipids.

A handheld probe is used to acquire measurements in subjects. The probe housing contains frequency domain, CW illumination fibers, CW detection fiber, and avalanche photodiode for frequency domain detection. In breast tissue, the DOSI instrument measures tissue properties between 1 and 5 cm below the skin. Measurements represent average optical properties for the measurement tissue volume, typically several centimeters cubed.

Subject Measurements. This study is a retrospective analysis conducted in early 2010 of a subset of subjects with newly diagnosed, operative, primary breast cancer measured with DOSI during their neoadjuvant chemotherapy treatment between 2005 and 2009. Because there was almost no data on chemotherapy monitoring with optical techniques before the initiation of this study, attempts were made to make exploratory measurements of subjects as frequently as possible during their treatment. The 23 subjects included in this study are those subjects who were measured with DOSI at a minimum of baseline and day 1 after their first infusion, and 17 patients were measured at least three times during their first week of treatment. One subject has bilateral disease, and therefore, a total of 24 tumors was monitored. All subjects provided informed consent and participated in this study under a clinical protocol approved by the Institutional Review Board at the University of California, Irvine (02-2306). Exclusion criteria included pregnant women and women who were less than 21 y old or more than 75 y old. All subjects were histologically diagnosed with invasive carcinoma before neoadjuvant treatment. Estrogen receptor (ER), progesterone receptor (PrR), and c-erbB2 (HER2) were immunohistochemically assessed from core biopsy. Positive HER2 status was confirmed using FISH analysis.

All subjects received neoadjuvant chemotherapy before surgical resection of tumors and were measured with the DOSI system before treatment (to establish a baseline measurement), 1 d after the start of treatment, and as many days as possible in the remaining first 7 d of treatment. Based on our previous findings, baseline measurements were obtained at least 10 d after diagnostic biopsies to minimize their impact on DOSI scans (4). Subjects were measured in a supine position. The DOSI probe was placed against the breast tissue, and sequential measurements were taken in a linear or rectangular grid pattern using 10-mm spacing. Measurements were taken to include the area of the underlying tumor determined by ultrasound and palpation as well as a margin of surrounding normal tissue. Contralateral normal breast measurements were collected from subjects with unilateral breast cancer.

Total measurement time varied between 20 min and 1 h per subject. Molar concentrations (ct) of oxyhemoglobin (ctO_2Hb), deoxyhemoglobin (ctHHb), water, and lipids were calculated at each measurement point. Maps (images) of oxyhemoglobin, deoxyhemoglobin, water, and lipids were constructed by a linear interpolation between measurement points. Repeat DOSI scans have been shown previously to be relatively insensitive to probe contact pressure fluctuations, displaying less than 5% average variation in test–retest studies of human subjects (5).

Fig. S1 shows a typical DOSI map created from discrete measurement points taken every 10 mm in a grid pattern over an 8 × 5-cm area of tissue containing a 34-mm invasive ductal carcinoma (IDC). This map shows a composite optical index of ctHHb, water, and lipids that has been previously shown to be useful for identifying tumors, and it is termed the tissue optical index (TOI) (6). The resulting map shows increased optical contrast over the tumor. Note that the DOS image shows tissue optical properties in the x–y plane (i.e., *en face*), whereas ultrasound shows x–z anatomic features.

Neoadjuvant Chemotherapy Regimen. The focus of this study concerned tumor functional changes that occurred after the first chemotherapy infusion; 20 of 23 subjects received doxorubicin (60 mg/m^2) and cyclophosphamide (600 mg/m^2; AC therapy) at their first infusion. Of the remaining three subjects, two received paclitaxel, carboplatin, and trastuzumab (Pac+Carb+Her) at first infusion, and one received paclitaxel, carboplatin, and bevacizumab (Pac+Carb+Bev) at first infusion. Details of treatments are described below and in Table S1.

Twenty of twenty-three subjects received AC therapy i.v. every 14 d for two to four cycles. This treatment was followed three to four cycles of weekly paclitaxel [80 mg/m^2; either cremophore-bound or albumin-bound (nab-paclitaxel)] and carboplatin (Pac+Carb). Subjects with positive HER2/neu status received concurrent trastuzumab therapy at a 4-mg/kg loading dose followed by a maintenance dose of 2 mg/kg weekly for 10–12 cycles. Seven subjects with negative HER2/neu status received a regimen of concurrent Pac+Carb combined with bevacizumab (10 mg/kg every 2 wk for five to six cycles). Seven subjects received pegfilgrastim support s.c. 24 h or later after the first chemotherapy dose and after day 1 DOSI measurements.

Briefly, these chemotherapy regimens are indicated as follows: AC alone (n = 1), AC followed by Pac+Carb (AC→Pac+Carb; n = 7), AC followed by Pac+Carb and trastuzumab (AC→Pac+Carb+Tras; n = 6), AC followed by Pac+Carb and bevacizumab (AC→Pac+Carb+Bev; n = 6), concurrent Pac+Carb and bevacizumab (Pac+Carb+Bev; n = 1), and concurrent Pac+Carb and trastuzumab (Pac+Carb+Tras; n = 2).

Criteria of Treatment Response. Treatment response criteria were similar to those criteria defined in the National Surgical Adjuvant Breast and Bowel Project protocol (7). Baseline tumor size was determined by clinical ultrasound or MRI dependent on availability. Final assessment of pathologic therapeutic response in breast tumor was determined from standard pathology. The histological response in the resected lymph nodes was not evaluated for treatment response. Criteria of treatment response

were previously described (6). Briefly, treatment response was stratified into a tertiary classification scheme of pathologic complete response (pCR), partial response (PR), and no response (NR). Subjects with no residual carcinoma after therapy were considered pCR. Subjects with a 50% or greater reduction in tumor size determined from the maximum tumor dimension were considered PR, and subjects with a less than 50% reduction were considered NR.

Analysis. To determine the change in oxyhemoglobin, deoxyhemoglobin, water, and lipids over the first week of treatment, the mean values of these quantities inside a region corresponding to the tumor were computed. This region was determined based on ultrasound, local increases in ctHHb and water, and decreases in lipids. This combination of metrics, designated as the TOI, has been previously shown to be a consistent indicator of tumor location (6). Mean values were also computed from contralateral normal breast measurements. Absolute and percent changes in ctO_2Hb, ctHHb, water, and lipids over the first week of treatment were statistically compared with their baseline values.

It is important to note that, because DOSI is not a tomographic instrument such as MRI or PET, surface measurements represent average tissue properties over a large volume, typically 10 cm^3, for the probe geometry used (8). This property of DOSI means that even measurements taken over a known tumor location include properties that may be averaged between tumor and surrounding tissue. Although previous studies have shown that DOSI measurements do produce sufficient contrast to localize tumors (9, 10), it is not possible at this time to fully separate the contributions of tumor tissue and immediately adjacent normal tissue on the dynamic changes observed in this study.

It was noted that, over the first week of treatment, changes occurred in both the magnitude and the spatial extent of elevated oxyhemoglobin values in the tumor region. To quantify the spatial expansion or contraction of these values, the number of discrete measurement points with values above a set threshold was computed at each measurement date for each subject. The threshold was calculated from the baseline measurement as the mean value in the normal tissue surrounding the tumor. If the number of measurement points above this threshold increased at subsequent measurement dates, then the spatial extent was determined to increase. If the number of measurement points decreased, then the spatial extent also decreased. Measurements were taken using 1-cm spacing in the x and y directions, and therefore, expansion and contraction of areas were described in units of centimeters squared and percent change from baseline.

A combined magnitude/spatial extent metric was calculated as the product of the mean tumor value and the number of measurement points above the threshold. This combined metric was compared with baseline values for each subject.

Generalized Estimating Equations. To take into account the correlation between values for oxyhemoglobin, deoxyhemoglobin, water, and lipids measured on different days for individual subjects, the generalized estimating equations (GEE) method was applied with subjects as clusters, an exchangeable correlation structure, and a normal model with an identity link function. Separate models were fit to longitudinal data with the outcome variables of oxyhemoglobin, deoxyhemoglobin, water, and lipids. Each outcome variable was represented as a percent change from baseline. Predictors included chemotherapy response (NR, PR, and pCR), treatment (cytotoxic, cytotoxic and bevacizumab, and cytotoxic and trastuzumab), and measurement day. Models were examined that included variables representing interactions between these predictors. Sensitivity analyses were performed to assess the effect of outliers on the main findings of the paper. Potential outliers were identified using cluster deletion diagnostics previously described for the GEE method in the work by Preisser and Qaqish (11). For each outcome, the studentized distance measure of the influence of the i^{th} cluster on overall model fit (MCLS statistic) was examined. For each outcome, clusters having an MCLS value above the 95th percentile for the statistic were further investigated with sensitivity analysis. Clusters were removed from the models to investigate the effect on SEs of parameter estimates. Clusters were removed if their exclusion led to a mean reduction in the SE of estimates for regression parameters, including the interaction between response group and measurement day. The statistical significance of comparisons between chemotherapy response groups for the main findings (e.g., the outcome of oxyhemoglobin on day 1 after infusion) was then compared between models including and excluding the identified outliers.

From the final GEE model for a given outcome and tissue type, the estimated percent change from baseline for the PR and pCR response groups, adjusted for covariates, was compared with the estimated change from baseline of the NR response group at each of the 7 measurement d. The Bonferroni method was applied to maintain an experimentwise significance level of 0.05, with a comparisonwise significance level of 0.00357. Additionally, for each outcome, the estimated percent change from baseline was compared between the two treatment groups at a significance level of 0.05.

Longitudinal GEE models also were fit to assess the relationship between change from baseline for each of the four outcomes and demographic and clinical variables including age, Scarff–Bloom–Richardson (SBR) grading status, histology type [IDC vs. invasive lobular carcinoma (ILC)], HER2 status, ER status, PR status, and body mass index, which were adjusted for variation in tissue type, treatment, response, and measurement day.

Finally, for patients that had measurements made on both tumor breast tissue and normal breast tissue, we computed the difference between the percent change from baseline for the normal breast tissue and the percent change from baseline for the tumor breast tissue. This difference was then treated as the outcome variable for a GEE model with predictors of response group, treatment group, measurement day, and interaction between treatment group and measurement day. Outliers were identified by examining cluster deletion diagnostics with the MCLS statistic, and sensitivity analyses were performed to determine the effect of outlying data points on the models. Comparison of tumor and normal tissue was made using the score statistic at a significance level of 0.05. These methods were applied for analysis of paired data for oxyhemoblobin, deoxyhemoglobin, lipids, and water.

One of twenty-three subjects had bilateral breast cancer; one tumor achieved a pCR, and the other achieved a PR. Because these tumors achieved different responses, they had different SBR grades, and it is known that bilateral tumors frequently have disparate biology (even in the same subject) (12), for purposes of the GEE analysis, these tumors were treated as having come from different subjects but with the same demographic and treatment information.

SI Results

Two subjects were identified as outlying clusters for the outcome of oxyhemoglobin, two subjects were identified as outlying clusters for the outcome of tumor deoxyhemoglobin, two subjects were identified as outlying clusters for the outcome for tumor lipids, and one subject each was identified as an outlying cluster for the outcomes of normal tissue oxyhemoglobin, normal tissue deoxyhemoglobin, normal tissue lipids, and normal tissue water. Outcomes of the model excluding outliers are shown in Table S3, and specific outliers are identified. The exclusion of outliers did improve the statistical significance of the main findings of the paper but did not change the overall conclusions. For example, the P values obtained comparing the difference in means for the

outcome of oxyhemoglobin change on day 1 between response groups are nominal P values with outliers for PR vs. NR = 2.0×10^{-12}, P value without outliers = 3.6×10^{-16}, nominal P values with outliers for pCR vs. NR = 2.5×10^{-6}, and P value without outliers = 1.6×10^{-13}. The results presented in the text include outliers.

1. Jakubowski D, Bevilacqua F, Merritt S, Cerussi A, Tromberg B (2009) Quantitative absorption and scattering specta in thick tissues using broadband diffuse optical spectroscopy. *Biomedical Optical Imaging*, eds Fujimoto JG, Farkas DL, (Oxford University Press), pp 330–355.
2. Bevilacqua F, Berger AJ, Cerussi AE, Jakubowski D, Tromberg BJ (2000) Broadband absorption spectroscopy in turbid media by combined frequency-domain and steady-state methods. *Appl Opt* 39:6498–6507.
3. Pham TH, Coquoz O, Fishkin JB, Anderson E, Tromberg BJ (2000) Broad bandwidth frequency domain instrument for quantitative tissue optical spectroscopy. *Rev Sci Instrum* 71:2500–2513.
4. Tanamai W, et al. (2009) Diffuse optical spectroscopy measurements of healing in breast tissue after core biopsy: Case study. *J Biomed Opt* 14:014024.
5. Cerussi A, et al. (2009) Effect of contact force on breast tissue optical property measurements using a broadband diffuse optical spectroscopy handheld probe. *Appl Opt* 48:4270–4277.
6. Cerussi A, et al. (2007) Predicting response to breast cancer neoadjuvant chemotherapy using diffuse optical spectroscopy. *Proc Natl Acad Sci USA* 104:4014–4019.
7. Rastogi P, et al. (2008) Preoperative chemotherapy: Updates of National Surgical Adjuvant Breast and Bowel Project Protocols B-18 and B-27. *J Clin Oncol* 26: 778–785.
8. Tromberg BJ, et al. (2005) Imaging in breast cancer: Diffuse optics in breast cancer: Detecting tumors in pre-menopausal women and monitoring neoadjuvant chemotherapy. *Breast Cancer Res* 7:279–285.
9. Cerussi A, et al. (2006) In vivo absorption, scattering, and physiologic properties of 58 malignant breast tumors determined by broadband diffuse optical spectroscopy. *J Biomed Opt* 11:044005.
10. Cerussi AE, et al. (2001) Sources of absorption and scattering contrast for near-infrared optical mammography. *Acad Radiol* 8:211–218.
11. Preisser JS, Qaqish BF (1996) Deletion diagnostics for generalised estimating equations. *Biometrika* 83:551–562.
12. Cavaliere A, Bellezza G, Scheibel M, Vitali R, Sidoni A (2004) Biopathological profile of multiple synchronous homolateral and bilateral breast cancers. *Pathol Res Pract* 200:9–12.

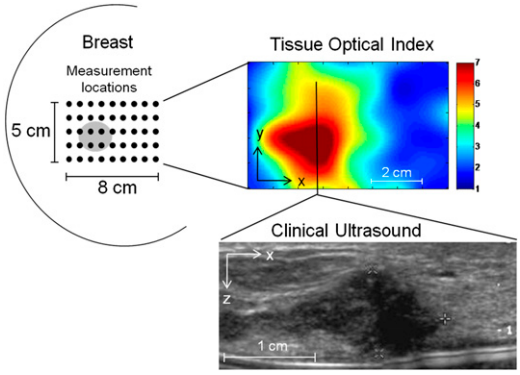

Fig. S1. Diagrammatic representation of the measurement procedure. DOSI measurements are taken in a grid or line pattern with a handheld probe in the *x–y* plane (*en face*). Measurements are taken every 10 mm over a tissue region previously determined by ultrasound and/or palpation to contain a tumor and include a surrounding normal margin. Measurements are also taken of the corresponding contralateral normal breast. In this example, an 8 × 5-cm region of tissue was measured containing a stage 2 IDC measured to be 34 mm in the greatest dimension. Maps of ctO_2Hb, ctHHb, water, and lipids are constructed from the measurement points. In this example, the map shows a composite metric termed the TOI, which is combination of ctHHb, water, and lipids; values above three are typical of tumors. A local increase in optical contrast is observed where the tumor is located. A clinical ultrasound measurement, which displays the tumor in the *x–z* plane, is shown for comparison.

Table S1. Subject characteristics and treatment regimens

Side	Age (y)	Size at max (mm)	TNM stage	Histology	SBR grade	ER	PrR	HER2	Treatment response	Treatment regimen	First day use of targeting therapy	Measured at least three times in week 1
Rt	43	40	T2N3M0	IDC	7	+	+	–	NR	AC→Pac+Carb	No	No
Rt	48	20	T1N1M0	ILC	6	+	+	–	NR	Pac+Carb+Bev	Yes	Yes
Rt	56	17	T1N0M0	IDC	4	+	+	–	NR	AC	No	Yes
Rt	57	20	T2N1M1	IDC	6	+	+	–	NR	AC→Pac+Carb	No	Yes
Rt	60	31	T2N1M0	IDC	7	–	–	+	NR	AC→Pac+Carb+Tras	No	Yes
Lt	71	34	T2N1M0	IDC	6	+	+	+	PR	Pac+Carb+Tras	Yes	Yes
Lt	55	20	T2N2M1	IDC	7	+	+	+	PR	AC→Pac+Carb+Tras	No	No
Lt	61	90	T4N2M0	IDC	8	+	+	–	PR	AC→Pac+Carb+Bev	No	No
Lt	63	60	T4N2M1	IDC	9	+	+	–	PR	AC→Pac+Carb+Bev	No	No
Rt	63	27	T2N1M0	IDC	5	ND	ND	ND	PR	AC→Pac+Carb+Bev	No	Yes
Rt	43	46	T2N0M0	ILC	6	+	–	–	PR	AC→Pac+Carb+Bev	No	Yes
Rt	33	43	T4N1M0	IDC	6	+	+	+	PR	AC→Pac+Carb+Tras	No	Yes
Lt	61	40	T2N0M0	ILC	6	+	+	–	PR	AC→Pac+Carb+Bev	No	Yes
Rt	41	38	T2N0M0	IDC	7	–	–	–	PR	AC→Pac+Carb+Bev	No	Yes
Lt	62	30	T4N2M0	IDC	7	+	+	–	PR	AC→Pac+Carb	No	Yes
Lt	41	35	T2N1M0	IDC	7	+	+	–	PR	AC→Pac+Carb	No	No
Lt	37	30	T3N1M0	IDC	ND	–	–	+	pCR	Pac+Carb+Tras	Yes	Yes
Lt	56	30	T3N1M0	IDC	7	–	–	+	pCR	AC→Pac+Carb+Tras	No	No
Lt	63	29	T2N2M0	IDC	8	+	+	–	pCR	AC→Pac+Carb+Bev	No	Yes
Rt	36	15	T1N1M0	IDC	7	+	+	–	pCR	AC→Pac+Carb	No	Yes
Lt	57	27	T2N0M0	IDC	7	+	+	+	pCR	AC→Pac+Carb+Tras	No	Yes
Lt	53	55	T3N1M0	IDC	6	–	–	+	pCR	AC→Pac+Carb+Tras	No	No
Rt	32	29	T2N1M0	IDC	8	–	–	–	pCR	AC→Pac+Carb	No	Yes
Lt	50	66	T4N2M0	ILC	ND	+	+	–	pCR	AC→Pac+Carb	No	Yes

AC, doxorubicin + cyclophosphamide; Bev, bevacizumab; Pac, paclitaxel; Carb, carboplatin; Tras, trastuzumab; ER, estrogen receptor; PrR, progesterone receptor; HER2, c-erbB2; IDC, invasive ductal carcinoma; ILC, invasive lobular carcinoma; Lt, left; Rt, right; ND, not described; NR, no response; PR, partial response; pCR, pathological complete response; SBR, Scarff–Bloom–Richardson score.

Table S2. Mean values and 95% confidence limits for percent change from baseline for 7 d after the start of chemotherapy in tumor and normal tissue for all outcomes as predicted by GEE models

		Tumor			Normal		
Outcome	Days	pCR	PR	NR	pCR	PR	NR
	1	44.25 (17.89, 70.6)	43.42 (24.12, 62.71)	−24.61 (−34.71, −14.51)	8.5 (−7.85, 24.85)	26.19 (−2.57, 54.96)	−4.33 (−10.5, 1.83)
	2	−1.4 (−20.46, 17.67)	22.76 (−8.43, 53.96)	−30.22 (−42.86, −17.59)	−2.43 (−15.09, 10.23)	3.17 (−11.28, 17.61)	−14.42 (−25.79,3.05)
	3	23.01 (6.63, 39.4)	14.81 (−14.59, 44.21)	−20.63 (−41.6, 0.34)	4.57 (−2.03, 11.17)	−9.74 (−24.19, 4.7)	−13.2 (−22.7, −3.7)
ctO_2Hb	4	−7.52 (−46.74, 31.7)	24.75 (−13.23, 62.72)	−29.22 (−46.29, −12.15)	−15.05 (−30.15, 0.05)	19.39 (−12.92, 51.7)	−19.78 (−32.3, −7.26)
	5	−15.68 (−40.26, 8.9)	16.6 (−17.3, 50.5)	−41.62 (−55.48, −27.77)	−13.62 (−32.85, 5.6)	7.71 (0.62, 14.8)	−25.33 (−29.2, −21.46)
	6	−4.05 (−21.81, 13.71)	26.2 (−19.9, 72.3)	−37.78 (−55.63, −19.94)	−3.09 (−17.57, 11.39)	6.12 (−8.05, 20.29)	−25.01 (−31.05, −18.97)
	7	−21.55 (−44.96, 1.85)	1.21 (−40.13, 42.54)	−49.38 (−63.24, −35.52)	−16.23 (−36.71, 4.26)	−11.19 (−24.51, 2.14)	−29.78 (−33.65, −25.91)
	1	15.1 (−13.92, 44.12)	−10.2 (−22.08, 1.67)	−20.22 (−31.46, −8.97)	−16.37 (−29.94, −2.79)	8.2 (−30.53, 46.92)	−11.82 (−17.86, −5.77)
	2	−13.83 (−23.56, −4.11)	−9.61 (−30.01, 10.79)	−20.31 (−35.84, −4.78)	−17.23 (−30.26, −4.19)	−12 (−29.04, 5.04)	−13.38 (−18.3, −8.46)
	3	−5.8 (−19.05, 7.45)	−54.69 (−73.99, -35.38)	−4.3 (−31.87, 23.28)	−13.91 (−22.18, −5.64)	−35.77 (−52.81, −18.73)	−11.43 (−19.6, −3.25)
ctHHb	4	17.73 (−8.4, 43.86)	13.28 (−7.99, 34.55)	−24.44 (−36.46, −12.42)	6.36 (−5.18, 17.91)	21.94 (−5.82, 49.71)	−5.39 (−11.1, 0.31)
	5	−5.81 (−33.71, 22.08)	8.46 (−11.59,28.52)	−38.16 (−51.32, −25)	4.64 (−18.93, 28.21)	7.6 (−38.68, 53.87)	−8.47 (−13.36, −3.59)
	6	−2.66 (−19.16, 13.84)	8.26 (−21.41, 37.92)	−26.99 (−48.36, −5.61)	3.26 (−12.07, 18.59)	−7.89 (−16.31, 0.53)	−6.34 (−10.8, −1.88)
	7	−4.52 (−20.17, 11.13)	17.95 (−16.29, 52.18)	−43.58 (−56.74, −30.42)	0.69 (−14.86, 16.24)	−3.14 (−32.33, 26.06)	−11.58 (−16.46, −6.69)
	1	6.55 (−0.98, 14.07)	3.6 (−3.31,10.51)	−1.54 (−8.65, 5.58)	−6.7 (−13.07, −0.33)	−1.26 (−4.67, 2.16)	−3.72 (−6.93, −0.52)
	2	−11.46 (−29.5, 6.57)	−16.04 (−28.01, −4.06)	−3.39 (−8.5, 1.73)	−2.49 (−4.46, −0.51)	−2.48 (−4.99, 0.03)	−3.78 (−5.18, −2.37)
	3	−23.48 (−29.75, −17.22)	−30.45 (−34.7, −26.2)	1.5 (−9.06, 12.06)	−8.56 (−11.26, −5.86)	−27.29 (−29.8, −24.78)	−1.77 (−6.76, 3.22)
Lipid	4	−21.77 (−45.66, 2.13)	−4.25 (−21.53, 13.02)	8.5 (−1.01, 18)	0.01 (−10.05, 10.07)	19.36 (−6.12, 44.83)	−0.34 (−2.2, 1.52)
	5	−19.57 (−35.55, −3.58)	2.91 (−10.14, 15.96)	14.12 (9.49, 18.76)	8.05 (1.94, 14.16)	6.25 (1.11, 11.39)	3.73 (1.05, 6.41)
	6	−6.67 (−24.27, 10.92)	−7.83 (−25.12, 9.46)	12.02 (8.81, 15.23)	−1.37 (−10.36, 7.63)	0.15 (−2.79, 3.09)	3.81 (2.55, 5.07)
	7	−7.06 (−19.55, 5.43)	6.26 (−0.1, 12.61)	14.2 (9.56, 18.83)	−2.07 (−9.21, 5.08)	0.92 (−3.44, 5.29)	−7.45 (−10.13, −4.77)
	1	6.99 (−6.55, 20.52)	−1.54 (−12.23, 9.15)	−5.88 (−18.34, 6.57)	−9.85 (−21.23, 1.52)	11.99 (−14.15, 38.12)	0.35 (−7.11, 7.8)
	2	−8.32 (−27.87, 11.22)	−12.91 (−46.84, 21.03)	3.02 (−12.43, 18.48)	4.26 (−6.9, 15.42)	0.79 (−9.97, 11.56)	4.09 (−2.16, 10.35)
	3	4.88 (−8.42, 18.18)	−23.69 (−34.17, −13.2)	17.34 (−9.18, 43.87)	−0.09 (−8.85, 8.68)	−23.04 (−33.8, −12.28)	6.53 (1.58, 11.48)
Water	4	3.01 (−13.09, 19.12)	15.54 (−2.52, 33.59)	−8.17 (−23.73, 7.4)	1.99 (−8.31, 12.28)	21.88 (−9.9, 53.67)	2.63 (−4.29, 9.56)
	5	−14.96 (−38.25, 8.33)	9.31 (−5.43, 24.05)	−20.65 (−38.39, −2.92)	1.17 (−14.4, 16.73)	−2.09 (−11.7, 7.51)	−1.09 (−6.7, 4.53)
	6	−5.49 (−19.64, 8.66)	4.42 (−22.24, 31.07)	1.75 (−34.55, 38.06)	1.19 (−12.78, 15.15)	−1.18 (−13.04, 10.69)	0.72 (−7.42, 8.87)
	7	−18.19 (−34.36, −2.02)	−9.79 (−27.96, 8.37)	−23.75 (−41.49, −6.01)	−5.61 (−18.17, 6.94)	0 (−17.87, 17.88)	−7.53 (−13.14, −1.91)

Table S3. Results of sensitivity analyses after exclusion of outliers

		Tumor			Normal		
Outcome	Days	pCR	PR	NR	pCR	PR	NR
ctO_2Hb*	1	27.66 (16.98, 38.34)	33.74 (24.26, 43.22)	−25.29 (−34.5, −16.07)	12.02 (−2.83, 26.88)	10.49 (2.22, 18.75)	−4.2 (−13.58, 5.18)
	2	−9.19 (-24.52, 6.15)	5.26 (−4.14, 14.66)	−29.64 (−39.64, −19.64)	−0.41 (−10.28, 9.45)	−4.04 (−9.87, 1.8)	−16.24 (−30.85, −1.63)
	3	16.49 (5.77, 27.2)	−0.9 (−10.3, 8.5)	−20.47 (−38.63, −2.31)	5.24 (−1.25, 11.74)	−16.95 (−22.78, −11.11)	−13.36 (−28.1, 1.38)
	4	10.64 (2.24, 19.05)	8.13 (−18.66, 34.93)	−29.33 (−49.74, −8.93)	−11.16 (−28.36, 6.04)	17.74 (−11.71, 47.18)	−21.17 (−30.29, −12.05)
	5	−28.4 (-42.07, −14.72)	−0.21 (−19.62, 19.2)	−44.05 (−56.56, −31.54)	−10.67 (−27.64, 6.29)	6.05 (1.64, 10.46)	−24.82 (−29.31, −20.33)
	6	−9.67 (-23.23, 3.9)	0.35 (−11.35, 12.04)	−39.34 (−55.4, −23.28)	−1.05 (−15.27, 13.17)	2.45 (−6.56, 11.46)	−23.18 (−26.98, −19.37)
	7	−19.31 (-38.82, 0.2)	−20.9 (−38.14, −3.66)	−51.81 (−64.31, −39.3)	−14.93 (−35.18, 5.33)	−16.26 (−26.17, −6.34)	−29.27 (−33.76, −24.78)
ctHHb†	1	−1.34 (-13.86, 11.18)	−14.2 (−25.3, −3.1)	−19.47 (−29.67, −9.28)	−11.69 (−22.55, −0.82)	−13.97 (−21.99, −5.95)	−11.81 (−21.55, −2.07)
	2	−15.89 (-26.43, −5.35)	−23.9 (−38.1, −9.7)	−18.95 (−34.34, −3.56)	−13.26 (−22.5, −4.02)	−18.77 (−28.11, −9.42)	−14.95 (−18.93, −10.98)
	3	−9.67 (-20.47, 1.13)	−67.26 (−81.46, −53.06)	−3.79 (−32.01, 24.42)	−9.58 (−16.64, −2.51)	−42.53 (−51.88, −33.19)	−11.65 (−14.86, −8.45)
	4	10.66 (-10.39, 31.71)	2.3 (−14.93, 19.53)	−23.62 (−34.76, −12.47)	10.15 (−2.47, 22.77)	19.07 (−14.69, 52.83)	−6.55 (−16.26, 3.15)
	5	−13.1 (-42.11, 15.9)	−2.29 (−18.23, 13.64)	−37.29 (−49.17, −25.42)	7.68 (−12.26, 27.62)	25.01 (−19.77, 69.79)	−8.12 (−14.72, −1.52)
	6	−3.32 (-18.43, 11.79)	−7.93 (−24.3, 8.45)	−27.16 (−45.89, −8.43)	6.67 (−8.07, 21.41)	−11.71 (−19.01, −4.42)	−4.92 (−10.53, 0.69)
	7	−4.97 (-20.15, 10.21)	−0.64 (−25.89, 24.61)	−42.72 (−54.59, −30.84)	3.23 (−11.03, 17.5)	−9.57 (−45.21, 26.08)	−11.23 (−17.82, −4.63)
Lipid‡	1	5.22 (-1.5, 11.95)	2.72 (−5.03, 10.47)	−0.21 (−5.89, 5.47)	−6.46 (−12.76, −0.16)	−0.11 (−3.16, 2.93)	−3.48 (−6.32, −0.64)
	2	−8.96 (-27.17, 9.26)	−14.63 (−26.78, −2.48)	−1.77 (−5.73, 2.19)	0.37 (−2.72, 3.45)	−2.98 (−5.41, −0.55)	−4.13 (−5.36, −2.9)
	3	−19.64 (-24.99, −14.28)	−29.39 (−34.57, −24.22)	2.03 (−6.28, 10.33)	−2.49 (−5.38, 0.4)	−27.79 (−30.23, −25.36)	−2.02 (−6.4, 2.36)
	4	−2.78 (-7.95, 2.38)	−3.23 (−19.52, 13.06)	9.72 (−1.09, 20.53)	−1.33 (−10.87, 8.2)	4.08 (−2.17, 10.32)	−1.29 (−4.58, 2)
	5	−9.66 (-20.84, 1.51)	3.25 (−9.6, 16.09)	15.91 (11.79, 20.03)	6.97 (−0.12, 14.05)	9.76 (7.92, 11.6)	3.97 (2.16, 5.79)
	6	2.27 (-9.51, 14.06)	−0.03 (−12.69, 12.62)	12.08 (8.42, 15.74)	−0.14 (−9.02, 8.73)	0.17 (−3.7, 4.04)	3.91 (2.45, 5.37)
	7	−2.88 (-14.67, 8.92)	8.4 (1.13, 15.67)	15.98 (11.86, 20.11)	−1.46 (−8.05, 5.14)	0.61 (−5.31, 6.54)	−7.21 (−9.02, −5.39)
Water§	1	6.99 (-6.55, 20.52)	−1.54 (−12.23, 9.15)	−5.88 (−18.34, 6.57)	−7.21 (−17.22, 2.8)	−2.47 (−10.62, 5.68)	0.25 (−7.44, 7.95)
	2	−8.32 (-27.87, 11.22)	−12.91 (−46.84, 21.03)	3.02 (−12.43, 18.48)	6.18 (−4.42, 16.79)	−2.9 (−10.79, 4.99)	3.21 (−4.23, 10.65)
	3	4.88 (-8.42, 18.18)	−23.69 (−34.17, −13.2)	17.34 (−9.18, 43.87)	3.45 (−5.77, 12.67)	−26.73 (−34.63, −18.84)	6.4 (−0.37, 13.17)
	4	3.01 (-13.09, 19.12)	15.54 (−2.52, 33.59)	−8.17 (−23.73, 7.4)	3.52 (−4.9, 11.93)	4.67 (−14.75, 24.09)	3.25 (−2.23, 8.74)
	5	−14.96 (-38.25, 8.33)	9.31 (−5.43, 24.05)	−20.65 (−38.39, −2.92)	2.26 (−11.74, 16.25)	1.37 (−8.32, 11.05)	0.71 (−3.7, 5.12)
	6	−5.49 (-19.64, 8.66)	4.42 (−22.24, 31.07)	1.75 (−34.55, 38.06)	2.53 (−11.33, 16.38)	−1.22 (−11.67, 9.22)	2.32 (−5.12, 9.75)
	7	−18.19 (-34.36, −2.02)	−9.79 (−27.96, 8.37)	−23.75 (−41.49, −6.01)	−4.51 (−16.03, 7.02)	5.37 (−7.06, 17.8)	−5.73 (−10.14, −1.32)

Mean values and 95% confidence limits for percent change from baseline for 7 d after the start of chemotherapy in tumor and normal tissue for all outcomes as predicted by GEE models.

*One PR and one pCR were excluded in the tumor group (rows 10 and 24 in Table S1, respectively). One PR was excluded in the normal group (row 7 in Table S1).

†One PR and one pCR were excluded in the tumor group (rows 10 and 24 in Table S1, respectively). One PR was excluded in the normal group (row 12 in Table S1).

‡One PR and one pCR were excluded in the tumor group (rows 14 and 17 in Table S1, respectively). One PR was excluded in the normal group (row 12 in Table S1).

§One PR was excluded in the normal group (row 12 in Table S1).

Table S4. Mean difference between percent change from baseline in DOSI measures for tumor and normal tissue and 95% confidence limits for the mean difference as predicted by GEE models

		Tumor − normal		
Outcome	Days	pCR	PR	NR
ctO_2Hb	1	38.91 (16.35, 61.48)	2.38 (−20.98, 25.73)	−20.5 (−27.42, −13.58)
	2	5.05 (−18.75, 28.85)	−5.59 (−23.46, 12.29)	−15.48 (−29.09, −1.86)
	3	25.49 (14.29, 36.7)	1.17 (−16.71, 19.04)	−5.14 (−22.67, 12.39)
	4	9.92 (−10.77, 30.61)	−14 (−39.01, 11)	−11.68 (−19.64, −3.71)
	5	4.21 (−35.16, 43.57)	−15.15 (−33.26, 2.96)	−20.77 (−30.79, −10.74)
	6	7.42 (−8.11, 22.94)	−15.09 (−32.24, 2.06)	−11.9 (−35.99, 12.19)
	7	3.29 (−7.86, 14.44)	−21.68 (−41.91, −1.44)	−24.08 (−34.1, −14.06)
ctHHb	1	39.2 (13.66, 64.74)	−25.87 (−62.29, 10.54)	−6.76 (−15.51, 1.99)
	2	4.97 (−15.46, 25.39)	−11.26 (−32.04, 9.51)	−5.74 (−16.9, 5.41)
	3	10.29 (−2.94, 23.51)	−30.85 (−51.63, −10.08)	8.93 (−13.02, 30.88)
	4	22.55 (5.29, 39.82)	−15.18 (−40.64, 10.27)	−17.43 (−27.95, −6.9)
	5	7.88 (−12.94, 28.69)	−5.26 (−55.32, 44.8)	−28.42 (−39.05, −17.79)
	6	0.44 (−16.69, 17.56)	−1.56 (−24.13, 21.01)	−18.5 (−37.93, 0.92)
	7	3.88 (−12.25, 20)	21.51 (−11.09, 54.1)	−30.73 (−41.36, −20.1)
Lipid	1	10.54 (0.22, 20.86)	2.15 (−2.41, 6.71)	2.24 (−4.63, 9.11)
	2	−1.67 (−14.04, 10.71)	−5.45 (−11.96, 1.07)	1.26 (−3.66, 6.18)
	3	−17.66 (−25.04, −10.28)	−2 (−8.51, 4.52)	3.57 (−6.28, 13.42)
	4	−23.12 (−43.75, −2.5)	−17.97 (−59.85, 23.92)	10.01 (3.26, 16.77)
	5	−27.29 (−46.89, −7.68)	−3.92 (−14.92, 7.08)	10.38 (5.3, 15.45)
	6	2.92 (−11.94, 17.79)	−7.03 (−30.42, 16.36)	7.78 (3.59, 11.97)
	7	−6.91 (−17.72, 3.91)	3.07 (−4.86, 11.01)	21.63 (16.55, 26.7)
Water	1	17.3 (4.63, 29.97)	−21.48 (−41.63, −1.33)	−6.05 (−12.62, 0.53)
	2	−4 (−15.88, 7.87)	1.11 (−4.58, 6.79)	−4.32 (−9.11, 0.47)
	3	6.6 (−0.53, 13.72)	−8.98 (−14.67, −3.3)	13.35 (−11.89, 38.59)
	4	3.52 (−3.87, 10.9)	−22.46 (−56.41, 11.5)	−19.45 (−27.79, −11.12)
	5	−3.02 (−10.1, 4.07)	0.43 (−8.26, 9.12)	−35.59 (−43.64, −27.55)
	6	−2.9 (−17.71, 11.92)	−14.03 (−26.33, −1.73)	0.07 (−49.72, 49.85)
	7	−6.01 (−16.35, 4.32)	−25.18 (−54.03, 3.67)	−32.25 (−40.3, −24.21)